Received: 4 May 2024 | Revised: 9 September 2024 | Accepted: 5 October 2024

DOI: 10.1111/bph.17395

THEMED ISSUE ARTICLE

DysRegNet: Patient-specific and confounder-aware dysregulated network inference towards precision therapeutics

Johannes Kersting[1] | Olga Lazareva[2,3,4,5] | Zakaria Louadi[2,6] | Jan Baumbach[6,7] | David B. Blumenthal[8] | Markus List[1,9]

[1]Data Science in Systems Biology, TUM School of Life Sciences, Technical University of Munich, Freising, Germany

[2]Chair of Experimental Bioinformatics, TUM School of Life Sciences, Technical University of Munich, Freising, Germany

[3]European Molecular Biology Laboratory, Genome Biology Unit, Heidelberg, Germany

[4]Division of Computational Genomics and Systems Genetics, German Cancer Research Center (DKFZ), Heidelberg, Germany

[5]Junior Clinical Cooperation Unit Multiparametric Methods for Early Detection of Prostate Cancer, German Cancer Research Center (DKFZ), Heidelberg, Germany

[6]Institute for Computational Systems Biology, University of Hamburg, Hamburg, Germany

[7]Department of Mathematics and Computer Science, University of Southern Denmark, Odense, Denmark

[8]Department Artificial Intelligence in Biomedical Engineering (AIBE), Friedrich-Alexander-Universität Erlangen-Nürnberg (FAU), Erlangen, Germany

[9]Munich Data Science Institute, Technical University of Munich, Garching, Germany

Correspondence
Markus List, Data Science in Systems Biology, TUM School of Life Sciences, Technical University of Munich, Freising, Germany.
Email: markus.list@tum.de

Funding information
European Commission, Grant/Award Numbers: 101057619, 777111; Bundesministerium für Bildung und Forschung, Grant/Award Numbers: 01ZX1908A, 031L0309A, 01ZX1910D; Villum Fonden, Grant/Award Number: 13154; Bavarian State Ministry of Science and the Arts; Deutsche Forschungsgemeinschaft, Grant/Award Number: 422216132; Swiss State Secretariat for Education, Research and Innovation (SERI), Grant/Award Number: 22.00115

Abstract

Background and Purpose: Gene regulation is frequently altered in diseases in unique and patient-specific ways. Hence, personalised strategies have been proposed to infer patient-specific gene-regulatory networks. However, existing methods do not scale well because they often require recomputing the entire network per sample. Moreover, they do not account for clinically important confounding factors such as age, sex or treatment history. Finally, a user-friendly implementation for the analysis and interpretation of such networks is missing.

Experimental Approach: We present DysRegNet, a method for inferring patient-specific regulatory alterations (dysregulations) from bulk gene expression profiles. We compared DysRegNet to the well-known SSN method, considering patient clustering, promoter methylation, mutations and cancer-stage data.

Key Results: We demonstrate that both SSN and DysRegNet produce interpretable and biologically meaningful networks across various cancer types. In contrast to SSN, DysRegNet can scale to arbitrary sample numbers and highlights the importance of confounders in network inference, revealing an age-specific bias in gene regulation in breast

Abbreviations: BRCA, breast invasive carcinoma; COAD, colon adenocarcinoma; GRN, gene regulatory network; HNSC, head and neck squamous cell carcinoma; HTRIdb, Human Transcriptional Regulation Interactions database; KIRC, kidney renal clear cell carcinoma; KIRP, kidney renal papillary cell carcinoma; LIHC, liver hepatocellular carcinoma; LUAD, lung adenocarcinoma; LUSC, lung squamous cell carcinoma; PRAD, prostate adenocarcinoma; SSN, sample-specific network; STAD, stomach adenocarcinoma; TCGA, The Cancer Genome Atlas Program; TF, transcription factor; THCA, thyroid carcinoma.

Johannes Kersting, Olga Lazareva and Zakaria Louadi contributed equally to this work.

cancer. DysRegNet is available as a Python package (https://github.com/biomedbigdata/DysRegNet_package), and analysis results for 11 TCGA cancer types are available through an interactive web interface (https://exbio.wzw.tum.de/dysregnet).

Conclusion and Implications: DysRegNet introduces a novel bioinformatics tool enabling confounder-aware and patient-specific network analysis to unravel regulatory alteration in complex diseases.

KEYWORDS

cancer and carcinogenesis, computational pharmacology, epigenetics, gene transcription, mathematical modelling, systems pharmacology

1 | INTRODUCTION

Gene regulatory network (GRN) inference methods model regulatory relationships, based on gene co-expression measures such as (conditional) mutual information or (partial) correlation (Chai et al., 2014). A directed network is typically created by limiting the inference to transcription factors (TFs) and their putative target genes. While methods such as GENIE3 (Huynh-Thu et al., 2010) or ARACNE (Margolin et al., 2006) identify static GRNs from gene expression data, dynamic methods can compare the co-expression under different conditions (Bhuva et al., 2019).

Differential expression and co-expression analysis methods designed to compare two groups or more (e.g. disease and control) typically cannot account for disease heterogeneity, identify disease subgroups or describe patient-specific dysregulation patterns. In contrast, methods identifying patient-specific gene expression aberrations in a one-against-all comparison can report sample-specific outlier genes (Cummings et al., 2017; Kremer et al., 2017). However, these approaches cannot pinpoint the source of the dysregulation. For instance, a mutated TF may not change in expression but still can behave differently in regulating its target genes, thus highlighting that co-expression should be considered at the single-patient level.

Some methods for studying patient-specific regulatory patterns have been proposed (Chen et al., 2023; Huang et al., 2021; Kuijjer et al., 2019; Lee, Huang, & Han, 2020; Liu et al., 2016; Maron et al., 2021; Park et al., 2019). Most methods calculate the Pearson correlation between two genes before and after adding/removing one sample. Some, such as SSN (X. Liu et al., 2016), evaluate the significance of this difference using transformations to *z*-scores or *P*-values. P-SSN (Huang et al., 2021) expands upon this technique by incorporating partial correlation to account for indirect interactions. LIONESS (Kuijjer et al., 2019) can be adapted to any network inference approach, returning a weighted adjacency matrix, but does not offer any significant assessment. SWEET (Chen et al., 2023) extends the LIONESS approach by incorporating a sample-to-sample correlation weight to account for variations in subpopulation sizes, but is limited to Pearson correlation as a network inference strategy. Nakazawa et al. (2021) defined an edge contribution value to extract subnetworks from Bayesian networks inferred from all samples, and used this approach successfully for cancer subtyping.

What is already known

- Patient-specific alterations in gene regulation play a key role in complex diseases.
- These alterations can be studied using patient-specific regulatory networks.

What does this study add

- We present DysRegNet, a tool for patient-specific and confounder-aware dysregulated network inference.
- DysRegNet is freely available as a Python package.

What is the clinical significance

- Patient-specific networks provide insights into complex diseases and might point to novel therapeutic targets.

We note that existing approaches cannot correct for confounders such as sex, age and origin of the sample, which can impact the analysis at a single sample level. Moreover, the leave-one-sample-out approach is computationally expensive, especially for large cohorts.

These limitations motivated us to develop DysRegNet, a method that first infers linear models from control samples, where the TF expression is considered the explanatory variable and the expression of its target gene is the response variable. Subsequently, we consider the residual for each patient sample to determine if the co-expression pattern deviates from the expected value. The linear model allows DysRegNet to correct for known covariates and to compute results (including significance) considerably faster than competing methods (Supporting Information Note 1). We show that DysRegNet can infer biologically meaningful patient-specific networks and compare them to results from the SSN method (Liu et al., 2016), a state-of-the-art representative of correlation-based methods.

2 | METHODS

2.1 | The statistical model behind DysRegNet

We define a reference network $N=(G,T,E)$, where G is a set of genes, $T\subseteq G$ is a set of TFs, and $E\subseteq T\times G$ is a set of edges connecting TFs $t\in T$ to target genes $g\in G$. The role of the reference network is to limit the search space for potentially dysregulated edges and to provide prior information about expected healthy regulations. We discuss possible choices for the template network in Section 4.3.

For every pair of connected nodes (t_i,g_j), the relationship between the expression profiles of a TF t_i and a target gene g_j can be modelled as

$$\widehat{E}^H(g_j)=\beta_0^H+\beta_1^H\cdot E^H(t_i)+\sum_{l=2}^{L}\left(\beta_l^H\cdot C_l^H\right), \tag{1}$$

where $E^H(t_i)$ is the expression of a TF t_i in a cohort of healthy controls; $\widehat{E}^H(g_j)$ is the expected expression of a target gene g_j in a cohort of control samples; $\left\{C_2^H,..,C_L^H\right\}$ is a set of available covariates such as age, ethnicity and sex; and $\left\{\beta_0^H,...,\beta_L^H\right\}$ are coefficients estimated with an ordinary least squares model.

An edge $e_{ij}=(t^i,g^j)$ is dysregulated for a patient p if the edge exists in the reference network N, and, for patient p, the expression of g_j cannot be reliably estimated using the model from Equation (1). Formally, this means that the expected expression of $\widehat{E}^p(g_j)=\beta_0^H+\beta_1^H\cdot E^p(t_i)+\sum_{l=2}^{L}(\beta_l^H\cdot C_l^p)$ is *significantly* different from the actual value of $E^p(g_j)$. This difference can be defined as a residual of the model, that is, $r_{ij}^p=E^p(g_j)-\widehat{E}^p(g_j)$, which can be converted to a z-score using the following transformation:

$$z_{ij}^p=\frac{r_{ij}^p-\overline{r_{ij}^H}}{\sigma\left(r_{ij}^H\right)}, \tag{2}$$

where $\overline{r_{ij}^H}$ and $\sigma\left(r_{ij}^H\right)$ are the mean and standard deviation of the control cohort residuals $r_{ij}^H=E^H(g_j)-\widehat{E}^H(g_j)$. The z-scores are converted to P-values using the standard normal distribution and subsequently corrected for multiple hypothesis testing regarding the number of patients with the Bonferroni correction procedure at a 0.01 significance level.

2.2 | Data and statistical analysis

The data and statistical analysis in this study comply with the recommendations of the *British Journal of Pharmacology* on experimental design and analysis in pharmacology (Curtis et al., 2022).

2.2.1 | Data preprocessing

All data from The Cancer Genome Atlas Program (TCGA) (comprising gene expression profiles based on bulk RNA-seq, methylation, mutation and sample metadata) were acquired from the XENA browser (https://xena.ucsc.edu/) (Goldman et al., 2020). We included 11 cancers with at least 30 control samples available (labelled 'Solid Tissue Normal'). We used $\log_2(tpm+0.001)$ normalised counts of the PANCAN cohort as a gene expression dataset (see Table S1 for the exact sample numbers). We retained only genes expressed in at least 80% of the patients of a cancer type. Subsequently, we standardised the expression data gene-wise based on the mean and standard deviation of the cancer-specific control samples.

The three sample-level confounders used for DysRegNet (sex, age and ethnicity) were obtained from the curated clinical data. Missing values for age were replaced with the mean age across all samples of a cancer type.

Illumina 450K DNA methylation array data was filtered for CpG sites associated with promoter regions (according to Illumina's annotation). We then calculated the mean of all methylation β-values associated with the same gene to obtain a methylation value for each gene in each sample.

Somatic mutations were mapped to their genes. In our analysis, we considered mutations of 12 different effect categories: missense, nonsense, intron, frameshift deletion, frameshift insertion, splice site, in-frame deletion, in-frame insertion, RNA, translation start site, non-stop mutation and large deletion.

2.2.2 | Reference networks

In our analyses, we used three types of reference networks: computationally inferred networks using GENIE3 (Huynh-Thu et al., 2010), an experimentally derived regulatory network from the Human Transcriptional Regulation Interactions database (HTRIdb) (Bovolenta et al., 2012) and a protein-protein interaction (PPI) network from STRING (Jensen et al., 2009).

GENIE3

GENIE3 uses an ensemble of trees to estimate the strength of the regulatory relationship between all possible TF-target gene pairs. A list of 1639 human TFs was used from Lambert et al. (2018) (http://humantfs.ccbr.utoronto.ca/) to limit the search space. To obtain cancer-specific reference networks, we ran the GENIE3 R package (https://github.com/aertslab/GENIE3, version 1.20.0) individually on the control samples of each cancer type. The shared network was derived by summing up the edge importance scores of all cancer-specific networks. For all GENIE3-inferred networks, we retained only the top 100,000 highest-scoring edges. We chose this cutoff to obtain networks that fall in between the relatively small HTRIdb and the much larger STRING network in terms of size.

HTRIdb

The Transcriptional Regulation Interactions database (http://www.lbbc.ibb.unesp.br/htri) is an open-access database for experimentally validated TF-target gene interactions. The database provides information about regulation interactions among 284 TFs and

18,302 target genes detected by 14 distinct techniques (Bovolenta et al., 2012), namely, chromatin immunoprecipitation, concatenate chromatin immunoprecipitation, CpG chromatin immunoprecipitation, DNA affinity chromatography, DNA affinity precipitation assay, DNase I footprinting, electrophoretic mobility shift assay, southwestern blotting, streptavidin chromatin immunoprecipitation, surface plasmon resonance and yeast one-hybrid assay, chromatin immunoprecipitation coupled with microarray (ChIP-chip) or chromatin immunoprecipitation coupled with deep sequencing (ChIP-seq).

STRING

The STRING database (http://string-db.org/) is dedicated to protein–protein interactions. It was included in our assessment for a fair comparison between DysRegNet and SSN (X. Liu et al., 2016), which was originally evaluated using the STRING network. Following the described methodology, we also considered high-confidence interactions with a combined score larger than 0.9, retaining a total of 197,969 edges. The combined score is an aggregate of seven channels (neighbourhood, fusion, co-occurrence, co-expression, experimental, database and text mining).

2.2.3 | Patient clustering

We evaluated the similarity between patient-specific networks by computing a pairwise overlap coefficient for the set of dysregulated edges, that is,

$$o(p_i,p_j)=\frac{|E_{p_i}\cap E_{p_j}|}{\min(|E_{p_i}|,|E_{p_j}|)}, \tag{3}$$

where E_{p_i} and E_{p_j} are sets of the dysregulated edges for patients i and j, respectively. The resulting similarity matrix was used to cluster the patients with spectral clustering implemented in scikit-learn (https://github.com/scikit-learn/scikit-learn, version 1.1.3) (Pedregosa et al., 2011).

We assigned cancer-type labels to the clusters using the Hungarian algorithm implemented in the Munkres Python package (https://github.com/bmc/munkres, version 1.1.4). The Hungarian algorithm (Kuhn, 1955) assigns a cancer-type label l_j to every cluster c_i by globally optimising for a cost function. In our case, we maximised the F1 scores:

$$\mathrm{F1}(c_i,l_j)=\frac{(2\cdot|P_{ci}\cap P_{lj}|)}{(2\cdot|P_{ci}\cap P_{lj}|+|P_{lj}\setminus P_{c_i}|+|P_{ci}\setminus P_{lj}|)}, \tag{4}$$

where P_{ci} is the set of patients in cluster c_i and P_{lj} is the set of patients with the true cancer-type label l_j. After assigning a label to each cluster, we calculated and reported the average F1 score across all label-cluster pairs.

2.2.4 | Dysregulation scores

We compute dysregulation scores to quantify the dysregulation of a gene (either as a TF or a target gene) in an individual patient. For a target gene g, the dysregulation score is defined as $\tilde{d}_p(g)=d_p^{\mathrm{in}}(g)\div d_R^{\mathrm{in}}(g)$ where $d_p^{\mathrm{in}}(g)$ is the in-degree of g in the dysregulated network of patient p and $d_R^{\mathrm{in}}(g)$ is the in-degree of g in the reference network. Analogously, for a transcription factor t, the dysregulation score is defined as $\tilde{d}_p(t)=d_p^{\mathrm{out}}(t)\div d_R^{\mathrm{out}}(t)$ where $d_p^{\mathrm{out}}(t)$ is the out-degree of t in the dysregulated network of patient p and $d_R^{\mathrm{out}}(t)$ is the out-degree of t in the reference network.

2.2.5 | DNA methylation local model

To model the relationship between promoter DNA methylation and target gene dysregulation, we used the following linear model:

$$\widehat{me}(g)=\beta_0^{me}+\beta_1^{me}\cdot\tilde{d}(g), \tag{5}$$

Here, $me(g)=[me_1(g),\ldots,me_P(g)]$ is the vector of the average (across CpGs) promoter DNA methylation (see Section 2.2.1) of target gene g for all P patients, and $\tilde{d}(g)=\left[\tilde{d}_1(g),\ldots,\tilde{d}_P(g)\right]$ is the vector of g's dysregulation scores. The slope coefficients β_1^{me} were tested for significance with the null hypothesis $H_0:\beta_1^{me}=0$. The P-values were then corrected using the Benjamini–Hochberg method.

The linear models were estimated using the ordinary least squares implementation in the statsmodels Python package (https://github.com/statsmodels/statsmodels, version 0.13.5).

2.2.6 | DNA methylation global model

While Equation (5) allows us to test every target gene individually, we also applied a linear mixed-effect model to investigate the global association between promoter methylation and dysregulation across all target genes in the reference network. For this purpose, we built a model with a random intercept coefficient for each target, assuming different baseline methylation levels:

$$\widehat{me}(G)=\beta_0^{me*}+\beta_1^{me*}\cdot\tilde{D}_G+\gamma_g^{me}, \tag{6}$$

where $me(G)$ are the average (across CpGs) promoter DNA methylation values for any $g\subseteq G$, $\tilde{D}_G=\left[\tilde{d}_1(g_1),..,\tilde{d}_P(g_1),\tilde{d}_1(g_2),..,\tilde{d}_P(g_2),...\right]$ are target gene dysregulation scores across all target genes and patients, and γ_g^{me} is a random intercept for each target gene. The slope coefficient β_1^{me*} was tested for significance with the null hypothesis $H_0:\beta_1^{me*}=0$.

The linear mixed-effect models were estimated using the implementation in the statsmodels Python package (https://github.com/statsmodels/statsmodels, version 0.13.5).

2.2.7 | Mutation local model

We tested the association between a dysregulation score for a TF and its mutation status using a logistic regression model:

$$logit\{P[mu(t)=1]\}=\beta_0^{mu}+\beta_1^{mu}\cdot\tilde{d}(t) \quad (7)$$

Here, $mu(t)=[mu_1(t),...,mu_P(t)]$ is a binary vector indicating the mutation status (1 indicates the presence of at least one mutation, 0 means no mutation) of the TF t for all P patients, and $\tilde{d}(t)=\left[\tilde{d}_1(t),...,\tilde{d}_P(t)\right]$ is the vector of t's dysregulation scores. The slope coefficient β_1^{mu} was tested for significance with the null hypothesis $H_0:\beta_1^{mu}=0$. The P-values were then corrected using the Benjamini–Hochberg method. We only tested TFs that were mutated in at least six patients and only considered cancer types with a least 30 TFs fulfilling this criterion.

The logistic regression models were estimated using the implementation in the statsmodels Python package (https://github.com/statsmodels/statsmodels, version 0.13.5).

2.2.8 | Mutation global model

To evaluate the global relationship between TF mutations and dysregulation, we used a logistic mixed-effect model with a random intercept coefficient for each TF, assuming different baseline mutation loads:

$$logit\{P[mu(T)=1]\}=\beta_0^{mu*}+\beta_1^{mu*}\cdot\tilde{D}_T+\gamma_t^{mu}, \quad (8)$$

where $mu(T)$ are binary mutation statuses for any $t\subseteq T$, $\tilde{D}_T=\left[\tilde{d}_1(t_1),..,\tilde{d}_P(t_1),\tilde{d}_1(t_2),..,\tilde{d}_P(t_2),...\right]$ are TF dysregulation scores, and γ_t^{mu} is a random intercept for every TF. β_1^{mu*} was tested for significance with the null hypothesis $H_0:\beta_1^{mu*}=0$. We only tested TFs that were mutated in at least six patients and only considered cancer types with a least 30 TFs fulfilling this criterion.

The logistic mixed-effect models were estimated using the implementation in the pymer4 Python package (https://github.com/ejolly/pymer4, version 0.8.0).

2.2.9 | Hypothesis testing for cancer stage analysis

We separated the samples of each cancer into two groups: an early-stage group (stage I) and a late-stage group (stage III or stage IV). For better separability, we excluded stage II samples from this analysis because they pose an intermediate setting that can resemble either stage I or III too closely. We conducted cancer stage analysis exclusively for types of cancer with a minimum of 30 patients in both groups to ensure the preservation of statistical power. We then performed a one-sided Mann–Whitney U test, implemented in scikit-learn (https://github.com/scikit-learn/scikit-learn, version 1.1.3) (Pedregosa et al., 2011), for every TF in the reference network to assess whether its dysregulation scores are larger in the late stage compared to the early-stage group. We corrected the obtained P-values for multiple testing with the Benjamini–Hochberg method.

To identify the TF most significantly dysregulated in late-stage cancers, we ranked TFs according to their cancer-type-specific P-values derived from the GENIE3 shared reference network. Then we selected the TF with the lowest average rank across all cancer types.

2.2.10 | Confounder impact analysis

To assess the impact of confounders, we obtained two-tailed P-values for the corresponding coefficients of DysRegNet's linear models based on the coefficient's t-statistic. These P-values can be interpreted as the probability that the coefficient is zero and thus has no predictive power.

We compared all models within a cancer type to identify target genes whose expression prediction is most affected by a specific confounder. We further reported the target gene from the model with the smallest P-value for the confounder in question.

Multi-label categorical confounders, such as ethnicity, resulted in multiple ($l-1$, where l is the number of different categories) coefficients/P-values per model, which, for visualisation purposes, were summarised in one distribution.

2.3 | SSN

SSN, described by Liu et al. (2016), calculates the correlation difference introduced by adding one case sample to a set of control samples. For each case sample and each pair of genes, the following score is computed:

$$Z=\frac{\Delta PCC_n}{\left(1-PCC_n^2\right)\div(n-1)}, \quad (9)$$

where $\Delta PCC_n=PCC_{n+1}-PCC_n$ is the difference between the Pearson correlation coefficients calculated on the control samples (PPC_n) and the control samples with one case sample (PCC_{n+1}), and n is the number of control samples. We further converted the Z-values into P-values with a Z-test, as described by Liu et al. Next, we corrected the P-values for multiple hypothesis testing using the Bonferroni method. We set a cutoff that defines a dysregulated edge at a corrected P-value of 0.01 or lower, equal to the cutoff selected for DysRegNet.

2.4 | Web interface

The dysregulated networks of the 11 studied TCGA cancers can be interactively explored using a web interface (https://exbio.wzw.tum.de/dysregnet), which was built with Plotly Dash (https://plotly.com/dash/, version 2.0.0), the Cytoscape.js (Franz et al., 2016) wrapper Dash Cytoscape (https://dash.plotly.com/cytoscape, version 0.2.0), Dash Bio (https://dash.plotly.com/dash-bio, version v0.2.0) and a

Neo4j database (https://neo4j.com/, version 5.11.0). We inferred the visualised networks using the GENIE3 shared reference network.

Because the underlying network is vast and highly connected, the interface is centred around individually selected query genes. Only the regulatory connections between those genes and their targets or sources are displayed to keep the resulting network compact and tidy. Further query genes can be added to expand the graph in directions of interest.

We displayed the fraction of patients with a dysregulation for each regulatory connection, which is directly depicted by the corresponding edge in the graph network. This metric also can be compared visually between different cancer types. Furthermore, the web interface incorporates information about the gene mutation frequency and mean promoter DNA methylation. Heatmaps allow the investigation of the DNA methylation status and the significance of a dysregulation on the patient level.

To prevent the underlying graph structure from becoming too large, the maximum number of displayed edges is capped, and edges can be filtered by their fraction of dysregulated patients and their type. In case a user is interested in the full, unfiltered graph, it can be downloaded as a CSV file.

The displayed network can be directly exported to the online systems medicine platform Drugst. One (Maier et al., 2024) to obtain drugs targeting the dysregulated genes.

2.5 | Python package

An implementation of DysRegNet as described in Section 2.1 is available as an easy-to-access Python package (https://exbio.wzw.tum.de/dysregnet). The linear regression modelling, as well as coefficient *P*-value and R^2-value calculation, was implemented based on the ordinary least squares implementation in the statsmodels Python package (https://github.com/statsmodels/statsmodels).

Our package also provides some additional features, which we did not use in this study for better comparability with SSN. This includes a goodness of fit filter to ignore edges with a low R^2 value and the normality filter (D'Agostino, 1971; Pearson, 1973) implemented in the SciPy Python package (https://github.com/scipy/scipy) to test the assumption of normally distributed control sample residuals. Furthermore, the Python package can distinguish between four possible scenarios of dysregulation shown in Figure S7: suppressed activation (1), amplified activation (2), amplified repression (3) and suppressed repression (4). The Python package can be used to only consider scenarios 1 and 4, which correspond to a reduced response towards the TF expression rather than an amplified one (scenarios 2 and 3).

2.6 | Nomenclature of targets and ligands

Key genes in this article are hyperlinked to corresponding entries in https://www.guidetopharmacology.org/ and are permanently archived in the Concise Guide to PHARMACOLOGY 2021/22 (Alexander et al., 2021).

3 | RESULTS

3.1 | Overview of the method

DysRegNet requires a reference GRN and expression data of two groups as input (Figure 1a). The reference network defines feasible interactions and reduces false positives. It can consist of experimentally confirmed (e.g. HTRIdb; Bovolenta et al., 2012) or computationally inferred interactions (e.g. using GENIE3 [Huynh-Thu et al., 2010] or ARACNE [Margolin et al., 2006]). The expression data have to be partitioned into two groups: patient and control samples. Control samples define healthy co-expression patterns, which are then used to detect dysregulations in the patient samples. Optionally, DysRegNet can use confounders, such as age or sex, to refine the models further.

Our method fits a linear regression model for every edge in the reference network using the control samples (Figure 1b). Specifically, we model the expression level of the TF as an explanatory variable to estimate the expression level of the target gene. Confounding factors serve as additional explanatory variables. After estimating the model parameters using Ordinary Least Squares, we compute the residual for every patient sample, that is, the difference between the predicted expression level of the target gene and the observed one. The residual is transformed into a *z*-score using the distribution of the control sample residuals for standardisation. This technique is comparable with an outlier detection task in regression analysis. After evaluating all patients, *z*-scores are transformed into *P*-values and corrected for multiple testing (see Section 2.1).

The output of our method is a list of predicted dysregulated edges for every patient, which can be integrated into a network with one or several connected components (Figure 1c). It is important to note that previous studies used the term 'patient-specific (or sample-specific) regulatory network'. We prefer to call it a patient-specific dysregulated network because we can only identify outliers with respect to the original GRN but not learn new edges or a gain of function specific to one sample.

DysRegNet is available as a Python package (https://github.com/biomedbigdata/DysRegNet_package), and analysis results for 11 TCGA cancer types can be interactively explored through a web interface (https://exbio.wzw.tum.de/dysregnet).

3.2 | Pan-cancer analysis to assess biological relevance

We evaluated DysRegNet using 11 cancer types available in TCGA (see Section 2.2.1) and compared the results to those obtained using SSN (see Section 4.4 for a justification for choosing SSN as the reference method in our benchmark). We carried out four analysis types:

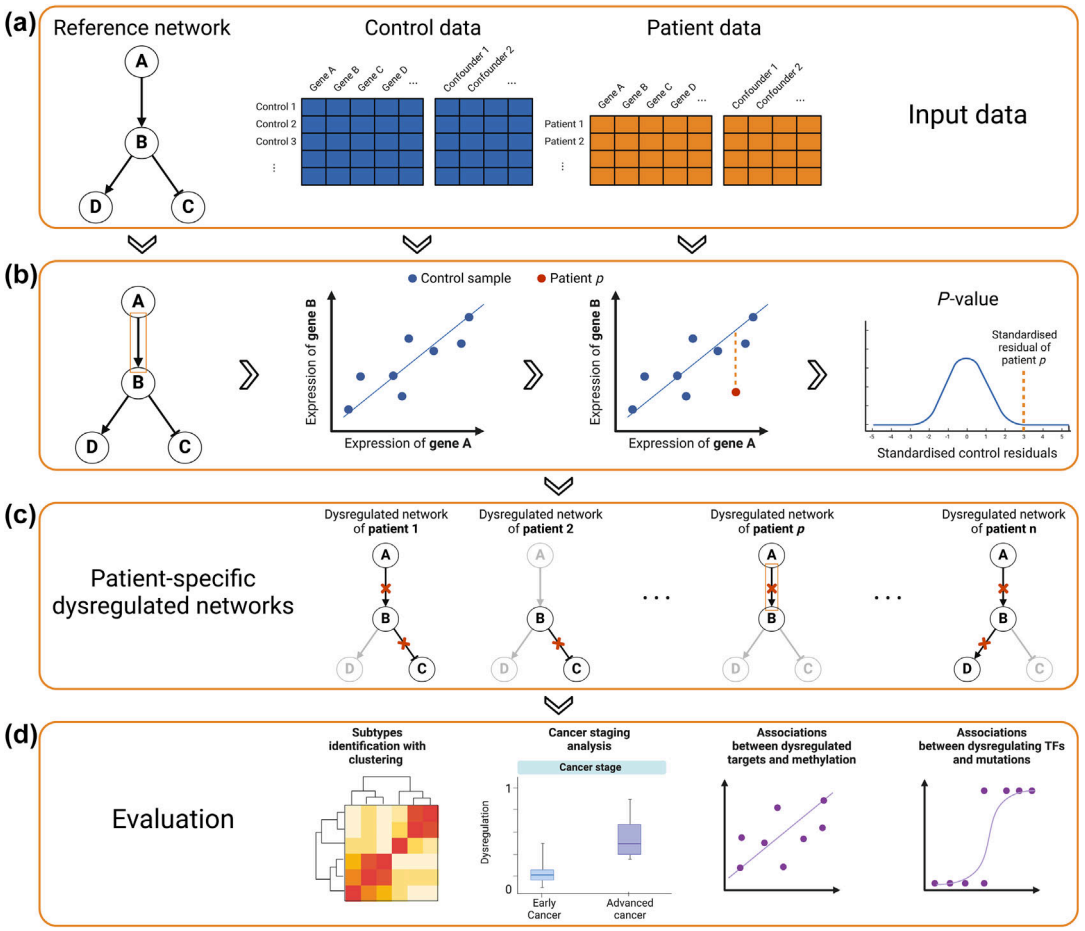

FIGURE 1 Overview of the method. (a) DysRegNet requires a reference network and expression data for control and patient samples as input. Additionally, multiple sample-level confounders can be provided. For illustration purposes, we assume the reference network has only three edges, with two activating and one repressing interaction. (b) Our method uses the control samples to infer a linear regression model for each edge in the reference network (the illustration focusses on the edge between genes A and B), modelling the expression level of the target gene based on the expression level of the TF and additional confounders if provided. Subsequently, we apply the obtained models to the patient samples, computing a residual for each patient sample. Based on the distribution of the control sample residuals, we assign a *P*-value to each patient residual. A low *P*-value suggests that the co-expression pattern of the patient significantly diverges from the control model, leading us to classify the edge as dysregulated. (c) Applying the described procedure to all patient samples and all edges in the reference network leads to the final output of DysRegNet: one network for each patient sample comprising all its dysregulated edges. (d) We evaluated the inferred patient-specific dysregulated networks using known cancer subtypes, cancer stage annotations, additional methylation and mutation data. Created with BioRender.com

patient clustering based on the computed networks, promoter methylation of dysregulated targets, dysregulation of mutated TFs and progression of dysregulation in different cancer stages (Figure 1d).

We used four types of reference networks for the evaluation: GENIE3 individual, GENIE3 shared, experimentally verified interactions from HTRIdb (referred to as *experimental*) and the STRING (Jensen et al., 2009) network. The GENIE3 networks were computationally generated using the GENIE3 method, where the individual network was inferred separately for each cancer type based on its specific control samples, and the shared network comprises the edge intersection of all individual networks. Thus, the shared network is the same for all analyses performed, whereas the individual networks are cancer-type specific. The STRING network is not limited to gene–regulatory interactions but considers protein–protein interactions (PPIs). We included a PPI network in the evaluation for a fair comparison with the SSN method that was evaluated using this network. We ran DysRegNet with three additional sample-level confounders, namely sex, age and ethnicity, which were all previously shown to be strong confounders in certain types of cancers (Kim et al., 2018; Laconi et al., 2020; Özdemir & Dotto, 2017).

For network topology visualisations, such as the number of edges and connected components, see Figures S3 and S4.

As outlined below, all four analyses suggest that the networks produced by DysRegNet capture biologically relevant signals and, in many cases, to a greater extent than those produced by SSN.

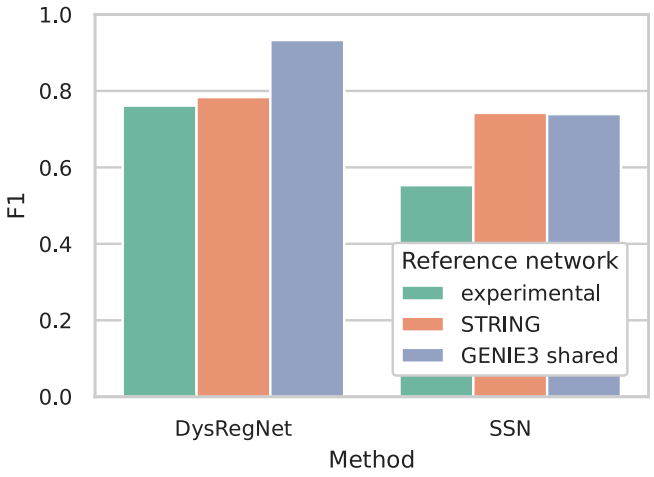

FIGURE 2 F1 scores assessing the agreement between the patients' cancer types and their assigned clusters. Higher is better.

3.2.1 | Patient-specific networks preserve characterising features of the cancer type

Even though our method infers an individual network for each patient, aiming to capture its potentially unique dysregulations, we expect similarities between patients of the same cancer type. We assume that patients with the same cancer type have similar dysregulated edges while patients with different cancers have fewer dysregulated edges in common. To investigate this, we evaluated the similarity between all individual patient networks across all cancer types by computing a pairwise overlap coefficient for their edge sets (see Section 2.2.3).

We then used spectral clustering to cluster the patients based on their similarity and assigned a label (i.e. the cancer type) to each cluster using the Hungarian algorithm, which maximises the F1 score of the label-cluster mapping (Kuhn, 1955). The evaluation was conducted using the shared GENIE3, HTRIdb and STRING networks. The individual (cancer-specific) GENIE3 networks were excluded because of high tissue specificity, making conclusions regarding the cancer specificity of the dysregulated networks impossible.

The final F1 scores for DysRegNet and SSN are shown in Figure 2. DysRegNet consistently performed better than SSN in this analysis, particularly when combined with the GENIE3 shared and experimental reference networks. This provides evidence that networks derived from DysRegNet can better capture cancer-type-specific characteristics.

3.2.2 | Target genes with methylated promoters are more likely to be dysregulated

DNA methylation plays a crucial role in controlling gene expression. For example, when CpG sites undergo methylation within the promoter region, it leads to repressed gene expression because TFs can no longer bind (Phillips, 2008). Therefore, gene promoter methylation is a diagnostic and prognostic cancer biomarker (Bouras et al., 2019). Even though changes in promoter methylation represent only one possible cause of dysregulation, we hypothesise that promoter methylation should be correlated with the dysregulation of a target gene across many samples.

Based on this hypothesis, we benchmarked SSN and DysRegNet with respect to the correlation of promoter methylation and patient-specific dysregulation. More specifically, we used linear regression to model the promoter methylation of target genes based on their overall dysregulation. To quantify this overall dysregulation of a target gene in a patient, we defined a dysregulation score as the number of its incoming edges in the patient-specific dysregulated network divided by the number of its incoming edges in the reference network (see Section 2.2.4). The dysregulation score, therefore, represents the proportion of TFs associated with a target gene that lost their ability to regulate it. Consequently, a high dysregulation score indicates that TFs generally lost the ability to regulate the target, which is what we would expect in cases where they can no longer bind to the promoter because of methylation. Note that while this would not affect TFs binding to enhancer regions, it suffices to show that dysregulation is related to changes in DNA methylation.

We built two different types of models: a local and a global one. While the local model tests every target gene individually, the global model tries to capture a trend across all target genes by including all of them in one mixed-effect model, adding the target gene as a random intercept (for details, see Sections 2.2.5 and 2.2.6). An illustration of the differences between the two models can be found in Figure S1.

Up to 20% of the tested target genes showed a significant link between their promoter methylation and dysregulation score (Figure 3) in both SSN and DysRegNet. The difference between both methods is relatively small. The results are further corroborated by global significance tests, revealing consistent patterns across all datasets except thyroid carcinoma (THCA), liver hepatocellular carcinoma (LIHC) and kidney renal clear cell carcinoma (KIRC), irrespective of the method or reference network used.

3.2.3 | Mutated TFs have more dysregulated targets

Mutations in TFs are associated with different types of cancer, such as lung cancer (Keshamouni, 2018), prostate cancer (Sun et al., 2005) and breast cancer (Takaku et al., 2020) as well as many others (Bushweller, 2019). We hypothesise that some mutated TFs may no longer be able to regulate their target genes, for example, because they lost the ability to bind to their motif.

As a measure, we defined a dysregulation score for TFs analogously to the dysregulation score for target genes used in the methylation analysis, the only difference being that we now focussed on outgoing instead of incoming edges. Thus, a high TF dysregulation score indicates that the TF had lost the ability to regulate many of its target genes, as expected for some mutated TFs. For this analysis, we

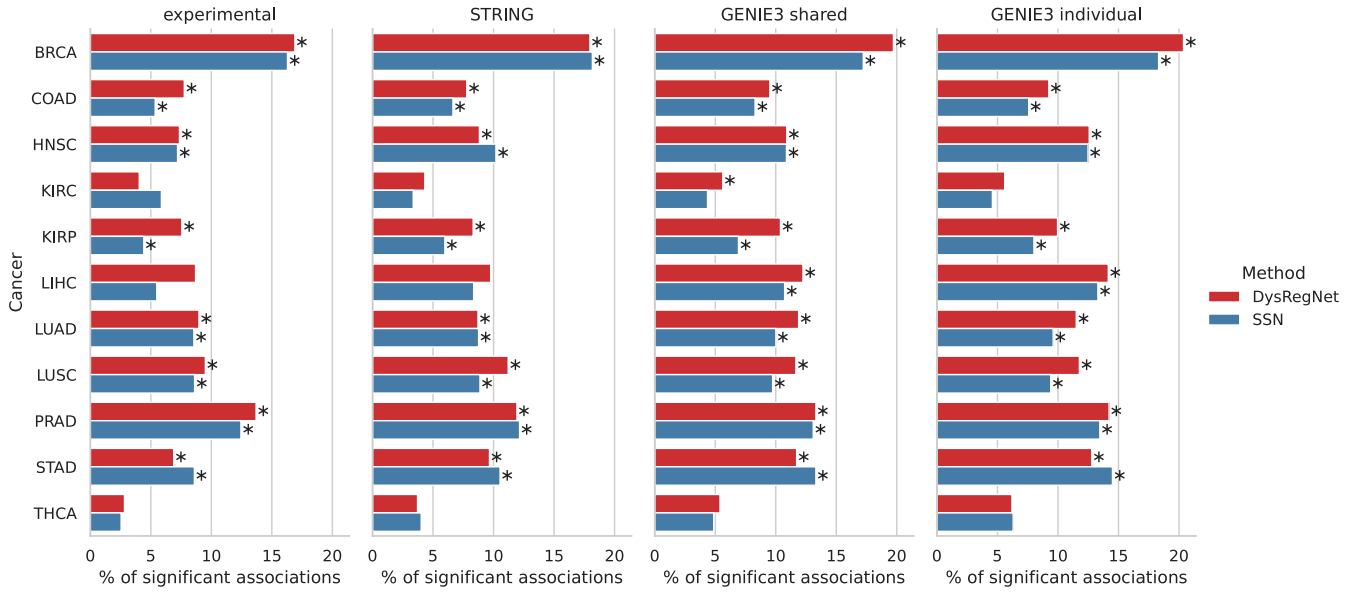

FIGURE 3 Percentages of target genes with a significant association (Benjamini–Hochberg adjusted *P*-value ≤ 0.05) between their promoter methylation and target gene dysregulation based on the local models. Bars with a star indicate that the global model (including all target genes) showed a significant association between promoter methylation and target dysregulation.

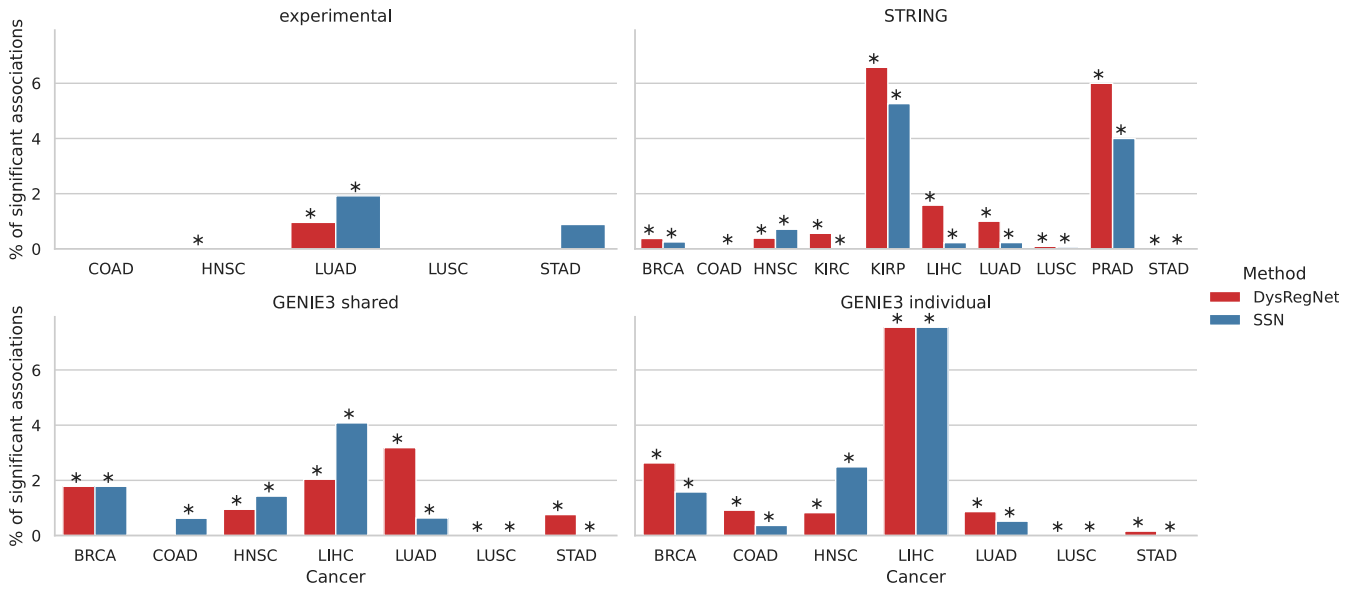

FIGURE 4 Percentages of TFs with a significant association (Benjamini–Hochberg adjusted *P*-value ≤ 0.05) between their mutation status and dysregulation. Bars with a star indicate a significant relationship based on the global model. Only cancer types with at least 30 TFs mutated in at least six patients were investigated.

modelled the mutation state of a TF based on its dysregulation score. Also, analogous to the methylation analysis, we performed tests using a local and a global model. However, because we treated the mutation state of a TF as a binary outcome, we switched from linear to logistic regression.

Figure 4 shows the results of the local- and global-scale analyses for all cancer types and reference network combinations investigated. The percentages of significant local models exhibit considerably lower and more variable values than those observed in the methylation tests. Nonetheless, the global tests reveal a correlation between mutated TFs and their dysregulation score across numerous scenarios. Again, DysRegNet and SSN perform similarly.

There are multiple factors explaining the disparity in the number of significant tests compared to the methylation analysis: A TF mutation is only one possible source of dysregulation, and only some specific mutations will affect the regulatory ability of TFs. Furthermore, most TFs were mutated only in a handful of patients, reducing the statistical power of our analyses.

Because of this, we still see the significant relationship between mutated TFs and their dysregulation indicated by global tests as further evidence of the biological meaningfulness of patient-specific networks.

3.2.4 | Patients with advanced stages of cancer exhibit increased dysregulation

Because of the accumulation of mutations (Hanahan & Weinberg, 2011) and progressing epigenetic reprogramming of gene regulation in cancer (Hanahan, 2022), we expect to observe increased gene dysregulation in the late stages of cancer compared to early stages.

To investigate this assumption, we divided patients into early-stage and late-stage groups for each cancer type (see Section 2.2.9). We then applied a one-sided Mann–Whitney *U* test to assess whether the dysregulation scores of TFs would be increased in the late-stage groups.

Except for colon adenocarcinoma (COAD) and breast invasive carcinoma (BRCA), large percentages of TFs showed increased dysregulation in late-stage patients, exceeding 80% for LIHC (Figure 5). Compared to SSN, DysRegNet-inferred networks generally contained more TFs with increased dysregulation in the advanced stages.

The TF, with the most significant dysregulation increase in late-stage patients across cancer types, was *ARNTL2*. *ARNTL2* was previously associated with cancer progression and aggressiveness in multiple cancer types (Mazzoccoli et al., 2012; Wang et al., 2020) and was shown to be a potential prognostic biomarker for treatment effectiveness (Ge et al., 2024). This shows that DysRegNet can be used to gain insights into oncological mechanisms and highlights its potential therapeutic value.

3.2.5 | Confounders significantly impact model inference

A distinguishing feature of DysRegNet is the ability to correct for sample-level confounders. To assess if including a patient's sex, age and ethnicity has an impact, we assessed the covariates model coefficients (Figure 6). Unsurprisingly, the TF expression coefficient produced the most significant *P*-values (see Section 2.2.10). However, the confounders noticeably impacted the regression models in various cancer types, such as age in BRCA, sex in LIHC, and ethnicity in stomach adenocarcinoma (STAD) and lung adenocarcinoma (LUAD).

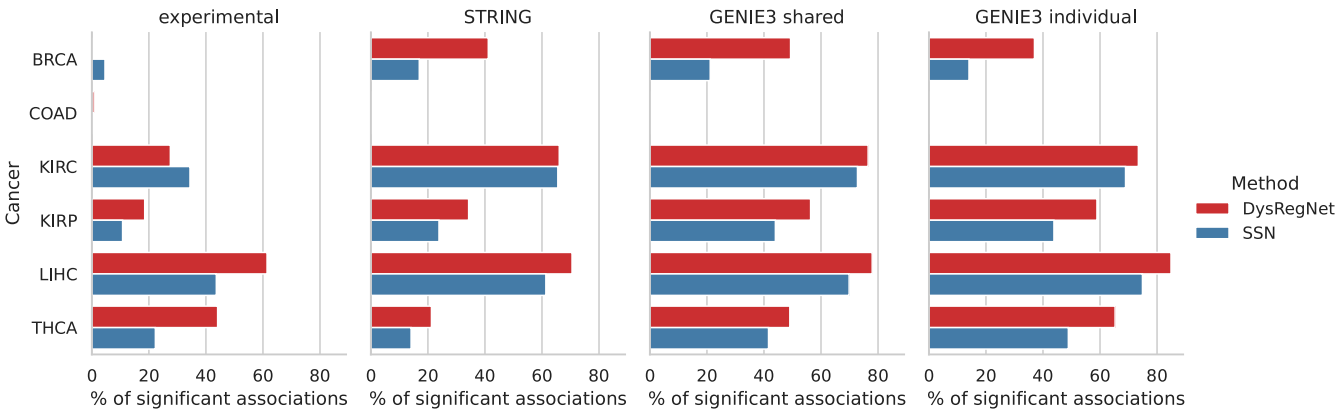

FIGURE 5 Percentages of TFs with significantly (Benjamini–Hochberg adjusted *P*-value ≤ 0.05) increased dysregulation in advanced cancer stages. Only cancer types with at least 30 patients in both (early-stage and late-stage) groups were tested.

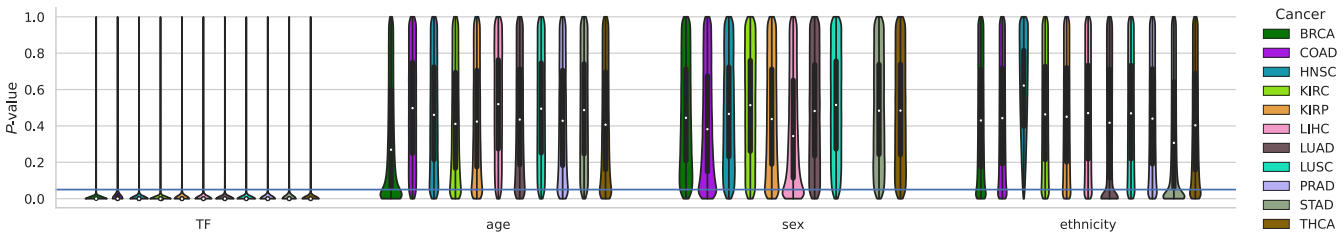

FIGURE 6 DysRegNet coefficient *P*-value distributions for different cancer types. The results are based on the GENIE3 shared reference network (see Figure S5 for the other reference networks). A single violin summarizes the *P*-values of a selected coefficient and cancer type across all linear models. The *P*-values of a confounder lacking meaningful predictive power will yield a random uniform distribution (e.g. age in colon adenocarcinoma). Conversely, influential confounders are expected to generate a disproportionate number of small *P*-values, manifesting as a pronounced concentration at the lower end of the *P*-value distribution, akin to a 'belly' in the violin plot (e.g. age in BRCA). Note that there are no *P*-values for sex in prostate adenocarcinoma (PRAD) because it inherently includes only male samples.

In BRCA, the age confounder had the strongest positive association (smallest *P*-value and positive coefficient) with the expression of the target gene ***NOX4***. This aligns with previous studies that have observed an increase in *NOX4* expression with age (Canugovi et al., 2019; Lee, Kim, et al., 2020; Liu et al., 2020). In LIHC, ***KDM5C*** was the target gene associated with the most significant *P*-value for sex. *KDM5C* is encoded on the X chromosome and is known to have higher expression in females than in males (Link et al., 2020; Samanta et al., 2022), which was reflected by the sign of the estimated coefficient.

This indicates that patient-level confounding factors influence the expression data, which DysRegNet can efficiently incorporate into its model construction and patient-specific network inference process.

4 | DISCUSSION

4.1 | Validity of model assumptions

Because DysRegNet is an outlier detection approach, it will be especially susceptible to technical biases. Additionally, because our method models gene pairs in isolation, it is limited in its ability to accurately capture complex network motifs, such as feedback loops. Furthermore, users should be aware that the method is built based on the following assumptions: (1) the target gene expression can be predicted based on TF expression using a linear regression model, and (2) the residuals of the linear model follow a normal distribution. The first assumption typically does not hold for PPI networks. Also, it will not hold for all TF-target gene pairs in a GRN. The activity of a TF can be influenced by many factors, such as interactions with other proteins, chromatin accessibility, or post-translational modifications; none of which are reflected in expression data (Filtz et al., 2014; Inukai et al., 2017). Additionally, other regulatory relationships in the data may be complex and nonlinear, making them difficult to model using linear regression. Because of these limitations, we recommend evaluating the goodness of fit of the underlying regression model before considering an edge as potentially dysregulated. Our Python package directly supports this by setting an R^2 cutoff. Similarly, we implemented a test to evaluate whether the residuals follow a normal distribution (D'Agostino, 1971; Pearson, 1973). This allows users to focus only on regulatory interactions that adhere to our second assumption.

4.2 | Importance of adjusting for confounders

Our results suggest that DysRegNet can account for typical confounders such as age and sex. However, it should be noted that these confounders do not seem to impact all data sets to the same extent. Age, for example, only affected the BRCA dataset. This finding is well-aligned with a recent study on the effect of demographic confounders on cohort-level network inference tools where age was identified as a strong confounder on network inference in BRCA based on data from two independent cohorts (TCGA and METABRIC) (Ketteler & Blumenthal, 2023). Given that BRCA has notably more control samples (113) than other cancer types (see Table S1), we assume that certain effects require a sufficiently large sample to be detected. Downsampling analysis that we performed further supports this hypothesis (see Figure S6). The same principle applies to categorical confounders such as sex or ethnicity, where aside from the overall sample size, each category must appear frequently enough to accurately estimate its effect. This suggests that DysRegNet could identify confounder impacts in other cancer types with sufficient sample sizes, but this still needs validation using larger datasets.

4.3 | Influence of different reference network

The initial reference network is a necessary input for DysRegNet. Our analysis considered three types: computationally inferred regulatory networks from GENIE3, an experimentally validated network from HTRIdb and a PPI network from STRING. We compared these networks in four different contexts: (i) patient clustering, (ii) promoter methylation of dysregulated target genes, (iii) dysregulation of mutated TFs and (iv) progression of dysregulation in different cancer stages.

The choice of the network depends on the research question. Users can expect computationally inferred networks to favour false positives, whereas experimentally validated networks may include more false negatives. We selected GENIE3 for computational network inference because it demonstrated its performance by winning the DREAM4 challenge (Huynh-Thu et al., 2010). Nevertheless, computational GRN inference remains an ongoing challenge, and we anticipate the emergence of improved methods in the future. Given that DysRegNet is flexible in terms of reference network choice, our approach can be used with any gold standard GRN available at that time.

In our analyses, the choice of the reference network seldom changed overall patterns. Our analyses produced better results when DysRegNet and SSN were combined with the computationally inferred GENIE3 networks, followed by the STRING and the experimentally validated network. A possible explanation is that the GENIE3 networks were constructed based on the same expression data used for the subsequent patient-specific network inference. Consequently, they more accurately reflect co-expression patterns observed in the data. As shown Figure S2, the R^2 values obtained by the linear regression models of DysRegNet were generally higher with the computationally inferred networks, indicating a better model fit.

Gene regulation differs across tissues and cell types (Kim-Hellmuth et al., 2020). Generic GRNs such as STRING and experimentally validated networks likely include regulatory interactions that may not be relevant to the tissues and datasets under study. In addition, these networks might encompass valid yet highly complex or nonlinear relationships, which are not easily captured by techniques such as linear regression or Pearson correlation. Both scenarios can lead to edges that cannot be reliably modelled with DysRegNet or the available data, potentially impacting the meaningfulness of the results. Because of this, the DysRegNet Python package provides an option

to only consider edges, which can be modelled with a certain R^2 value or higher.

Furthermore, it is important to note that the STRING network violates some of our modelling assumptions. For DysRegNet, we expect a gene regulatory reference network of directed TF–target gene relationships. However, the edges in the STRING network are neither directed nor are they actual TF–target gene pairs. While the overall co-expression modelling approach may still be valid, as we expect co-expression patterns between interacting proteins, our downstream measurements, such as dysregulation scores for TFs and target genes, lose interpretability.

4.4 | Evaluation

We evaluated our approach against the original single-sample GRN inference method SSN. Although we compared our method only to this approach, numerous other methods adopted a comparable procedure. Lee et al. (2020) extended the SSN approach by integrating multi-omics data such as copy number variation or DNA methylation. Because of the high similarity of methods and lack of public source code, a circumstance shared with Nakazawa et al. (2021), we did not include those methods in the evaluation. Furthermore, the available code of P-SSN (Huang et al., 2021) requires a special reference network with a list of potentially indirectly interacting genes for each edge. Because P-SSN does not use standard regulatory networks as input, a proper comparison with DysRegNet was impossible.

While DysRegNet identifies dysregulation compared to a healthy background, LIONESS (Kuijjer et al., 2019) and SWEET (Chen et al., 2023) do not utilise a dedicated set of control samples. This is a clear advantage for experiment designs with no controls. However, their patient-specific networks cannot be interpreted as dysregulated networks and must be analysed in the context of all other samples. Because of this difference in the result interpretation, we did not include them in our evaluation. The right tool choice depends on the question and the availability of control samples, which are often not available at a sufficient number (at least 20 samples are needed for a robust co-expression analysis [Ballouz et al., 2015]). For studies without controls, utilising independent tissue-specific expression data of healthy individuals can be an alternative. Park et al. (2019), for instance, employ a methodology closely related to the SSN approach where they leverage GTEx (GTEx Consortium, 2013) data. However, cross-study batch effects need to be accounted for in this case.

Despite recent attempts to systematically compare various sample-specific network inference methods (Chen et al., 2023; Deschildre et al., 2024), a proper evaluation remains a major challenge. We considered a variety of cancer expression datasets and networks across different complementary scenarios. Overall, our results indicate that DysRegNet and SSN produce biologically meaningful results. However, our evaluation is limited by the absence of ground truth and discrepancies in interpreting the networks generated by different methods (De Marzio et al., 2023). For example, we expect a higher percentage of dysregulated TFs in advanced cancer stages, while the true fraction or upper limit is unknown. Similarly, SSN networks generally comprise more dysregulated edges than those of DysRegNet, even though we used the same *P*-value cutoff and multiple testing correction procedures for both methods (see Figure S3). While this could suggest that DysRegNet generates fewer false positives, we cannot prove this without knowing the ground truth.

4.5 | Outlook

A promising direction for further research is a more in-depth investigation of the connection between dysregulations and mutations. This study investigated whether mutated TFs will be more frequently involved in dysregulation. However, unlike in the promoter methylation analysis, the association between dysregulation and mutations was less visible. We found significant associations for 7% of the tested TFs at most. Our analysis did not consider that not every somatic mutation will affect the regulatory function of a TF. A more specific analysis could focus on known or patient-specific mutations within the DNA-binding domains of TFs in the promoter or enhancer regions of target genes and model their impact on expression changes (Baumgarten et al., 2024). Furthermore, somatic mutations in cancer frequently affect the splice site and can cause isoform switches (Climente-González et al., 2017; Louadi et al., 2021). Our analysis was performed at the gene level, but a deeper analysis at the isoform or transcript level would help explain a larger fraction of the identified dysregulated edges.

Another interesting application of the method is in studying rare and undiagnosed diseases, where the focus is often on the unique differences of a single sample. The current rate of genetically diagnosed rare disorders is approximately 25% to 50% (Cummings et al., 2017). Thus, DysRegNet provides a novel opportunity to expand our knowledge of such disorders.

State-of-the-art GRN inference methods are increasingly adopting multi-omics approaches, such as integrating chromatin accessibility data alongside expression data. Expanding DysRegNet to incorporate multi-omics data presents an exciting direction for future research. This enhancement would enable our method to more accurately model regulatory relationships and thus identify dysregulation for interactions that are challenging to capture using expression data alone.

Single-patient network extraction is a promising research direction towards precision medicine as it highlights potential treatment targets in a personalised fashion. A plethora of computational methods have been developed for drug target identification and drug repurposing (Katsila et al., 2016). Many of these methods already use networks as input (Hartung et al., 2022; Sadegh et al., 2020, 2021) and embrace concepts of network pharmacology (Nogales et al., 2022). Typically, such methods extract disease modules after connecting patient- or disease-specific seed genes. Currently, seed gene selection is typically based on literature or patient-specific mutation or expression profiles. To our knowledge, patient-specific dysregulation and co-expression analysis have thus far not been employed to identify seed genes, suggesting a promising direction for further research.

5 | DISCUSSION AND CONCLUSIONS

Aberrant TF regulation is an important mechanism in complex diseases such as cancer. Rather than focussing on the aberrant expression of TFs or their target genes, it is worthwhile to study which specific interactions of a TF are affected to gain a more detailed insight into the underlying pathomechanisms. Many molecular changes can lead to the same outcome; hence, it is vital to study dysregulation in a patient-specific, or sample-specific, manner. With DysRegNet, we present a novel approach that delineates individual TF-regulatory changes in relation to a control cohort. In contrast to competing methods, DysRegNet uses linear models to account for confounders and residual-derived *z*-scores to assess significance. Because of the latter, DysRegNet scales efficiently to an arbitrary number of samples. We have shown that DysRegNet results are robust across template networks and produce meaningful insights into cancer biology. DysRegNet may hence serve as a precision medicine tool for identifying drug targets in oncology and beyond.

AUTHOR CONTRIBUTIONS

Johannes Kersting: Conceptualisation (lead); Formal analysis (lead); Methodology (lead); Software (lead); Visualisation (lead); Writing—original draft-Lead. **Olga Lazareva:** Conceptualisation (lead); Formal analysis (lead); Methodology (lead); Software (supporting); Visualisation (supporting); Writing—original draft (lead). **Zakaria Louadi:** Conceptualisation (lead); Formal analysis (lead); Methodology (lead); Software (equal); Visualisation (supporting); Writing—original draft (lead). **Jan Baumbach:** Conceptualisation (supporting); Methodology (supporting). **David Blumenthal:** Conceptualisation (supporting); Methodology (supporting); Writing—review and editing (supporting). **Markus List:** Conceptualisation (lead); Methodology (lead); Project administration (lead); Supervision (lead); Writing—original draft (supporting); Writing—review and editing (lead).

ACKNOWLEDGEMENTS

The results shown here are in whole or part based upon data generated by the TCGA Research Network: https://www.cancer.gov/tcga. Contributions from Z. L. J. B. and M. L. are funded by the German Federal Ministry of Education and Research (BMBF) within the framework of the e:Med research and funding concept [grant 01ZX1908A (Sys_CARE)]. Contributions by O.L. are funded by the Bavarian State Ministry of Science and the Arts within the framework coordinated by the Bavarian Research Institute for Digital Transformation (bidt, Doctoral Fellow). The project received funding from the Deutsche Forschungsgemeinschaft (DFG, German Research Foundation) [422216132]. This project has received funding from the European Union under grant agreements No. 101057619 and No 777111. Views and opinions expressed are, however, those of the author(s) only and do not necessarily reflect those of the European Union or European Health and Digital Executive Agency (HADEA). Neither the European Union nor the granting authority can be held responsible for them. This work was also partly supported by the Swiss State Secretariat for Education, Research and Innovation (SERI) under contract No. 22.00115. Furthermore, this work was supported by the German Federal Ministry of Education and Research (BMBF) within the framework of the e:Med research and funding concept (grant 01ZX1910D). JB was partially funded by his VILLUM Young Investigator Grant nr. 13154. D.B.B. was supported by the German Federal Ministry of Education and Research (BMBF) within the framework of the CompLS research and funding concept [grant 031L0309A (NetMap)]. Open Access funding enabled and organized by Projekt DEAL.

CONFLICT OF INTEREST STATEMENT

Z.L. has been an employee of Illumina, Inc. since September 2022. The authors declare no conflicts of interest.

DATA AVAILABILITY STATEMENT

The datasets and computer code produced in this study are available in the following databases:

- Expression, mutation, methylation and sample metadata: TCGA Pan-Cancer (PANCAN) cohort, XENA browser (https://xenabrowser.net/datapages/)
- PPI network: STRING database (http://string-db.org/)
- Experimentally validated regulatory network: Transcriptional Regulation Interactions database (originally obtained from http://www.lbbc.ibb.unesp.br/htri, currently available at https://rescued.omnipathdb.org/)
- List of human TFs: http://humantfs.ccbr.utoronto.ca/
- Python package: GitHub (https://github.com/biomedbigdata/DysRegNet_package)
- Analysis scripts: GitHub (https://github.com/biomedbigdata/DysRegNet_workflow)

DECLARATION OF TRANSPARENCY AND SCIENTIFIC RIGOUR

This Declaration acknowledges that this paper adheres to the principles for transparent reporting and scientific rigour of preclinical research as stated in the BJP guidelines for Design and Analysis, and as recommended by funding agencies, publishers and other organisations engaged with supporting research.

ORCID

Johannes Kersting https://orcid.org/0000-0002-3882-0093
Olga Lazareva https://orcid.org/0000-0001-9546-7807
Zakaria Louadi https://orcid.org/0000-0003-4763-0264
Jan Baumbach https://orcid.org/0000-0002-0282-0462
David B. Blumenthal https://orcid.org/0000-0001-8651-750X
Markus List https://orcid.org/0000-0002-0941-4168

REFERENCES

Alexander, S. P., Kelly, E., Mathie, A., Peters, J. A., Veale, E. L., Armstrong, J. F., Faccenda, E., Harding, S. D., Pawson, A. J., Southan, C., Buneman, O. P., & Zolghadri, Y. (2021). The Concise Guide to PHARMACOLOGY 2021/22: Introduction and other protein

targets. *British Journal of Pharmacology*, *178*(Suppl 1), S1–S26. https://doi.org/10.1111/bph.15537

Ballouz, S., Verleyen, W., & Gillis, J. (2015). Guidance for RNA-seq co-expression network construction and analysis: Safety in numbers. *Bioinformatics*, *31*(13), 2123–2130. https://doi.org/10.1093/bioinformatics/btv118

Baumgarten, N., Rumpf, L., Kessler, T., & Schulz, M. H. (2024). A statistical approach for identifying single nucleotide variants that affect transcription factor binding. *IScience*, *27*(5), 109765. https://doi.org/10.1016/j.isci.2024.109765

Bhuva, D. D., Cursons, J., Smyth, G. K., & Davis, M. J. (2019). Differential co-expression-based detection of conditional relationships in transcriptional data: Comparative analysis and application to breast cancer. *Genome Biology*, *20*(1), 236. https://doi.org/10.1186/s13059-019-1851-8

Bouras, E., Karakioulaki, M., Bougioukas, K. I., Aivaliotis, M., Tzimagiorgis, G., & Chourdakis, M. (2019). Gene promoter methylation and cancer: An umbrella review. *Gene*, *710*, 333–340. https://doi.org/10.1016/j.gene.2019.06.023

Bovolenta, L. A., Acencio, M. L., & Lemke, N. (2012). HTRIdb: An open-access database for experimentally verified human transcriptional regulation interactions. *BMC Genomics*, *13*(1), 405. https://doi.org/10.1186/1471-2164-13-405

Bushweller, J. H. (2019). Targeting transcription factors in cancer—From undruggable to reality. *Nature Reviews. Cancer*, *19*(11), 611–624. https://doi.org/10.1038/s41568-019-0196-7

Canugovi, C., Stevenson, M. D., Vendrov, A. E., Hayami, T., Robidoux, J., Xiao, H., Zhang, Y.-Y., Eitzman, D. T., Runge, M. S., & Madamanchi, N. R. (2019). Increased mitochondrial NADPH oxidase 4 (NOX4) expression in aging is a causative factor in aortic stiffening. *Redox Biology*, *26*, 101288. https://doi.org/10.1016/j.redox.2019.101288

Chai, L. E., Loh, S. K., Low, S. T., Mohamad, M. S., Deris, S., & Zakaria, Z. (2014). A review on the computational approaches for gene regulatory network construction. *Computers in Biology and Medicine*, *48*, 55–65. https://doi.org/10.1016/j.compbiomed.2014.02.011

Chen, H.-H., Hsueh, C.-W., Lee, C.-H., Hao, T.-Y., Tu, T.-Y., Chang, L.-Y., Lee, J.-C., & Lin, C.-Y. (2023). SWEET: A single-sample network inference method for deciphering individual features in disease. *Briefings in Bioinformatics*, *24*(2), bbad032. https://doi.org/10.1093/bib/bbad032

Climente-González, H., Porta-Pardo, E., Godzik, A., & Eyras, E. (2017). The functional impact of alternative splicing in cancer. *Cell Reports*, *20*(9), 2215–2226. https://doi.org/10.1016/j.celrep.2017.08.012

Cummings, B. B., Marshall, J. L., Tukiainen, T., Lek, M., Donkervoort, S., Foley, A. R., Bolduc, V., Waddell, L. B., Sandaradura, S. A., O'Grady, G. L., Estrella, E., Reddy, H. M., Zhao, F., Weisburd, B., Karczewski, K. J., O'Donnell-Luria, A. H., Birnbaum, D., Sarkozy, A., Hu, Y., … MacArthur, D. G. (2017). Improving genetic diagnosis in Mendelian disease with transcriptome sequencing. *Science Translational Medicine*, *9*(386), eaal5209. https://doi.org/10.1126/scitranslmed.aal5209

Curtis, M. J., Alexander, S. P. H., Cirino, G., George, C. H., Kendall, D. A., Insel, P. A., Izzo, A. A., Ji, Y., Panettieri, R. A., Patel, H. H., Sobey, C. G., Stanford, S. C., Stanley, P., Stefanska, B., Stephens, G. J., Teixeira, M. M., Vergnolle, N., & Ahluwalia, A. (2022). Planning experiments: Updated guidance on experimental design and analysis and their reporting III. *British Journal of Pharmacology*, *179*(15), 3907–3913. https://doi.org/10.1111/bph.15868

D'Agostino, R. B. (1971). An omnibus test of normality for moderate and large size samples. *Biometrika*, *58*(2), 341–348. https://doi.org/10.1093/biomet/58.2.341

De Marzio, M., Glass, K., & Kuijjer, M. L. (2023). Single-sample network modeling on omics data. *BMC Biology*, *21*(1), 296. https://doi.org/10.1186/s12915-023-01783-z

Deschildre, J., Vandemoortele, B., Loers, J. U., De Preter, K., & Vermeirssen, V. (2024). Evaluation of single-sample network inference methods for precision oncology. *Npj Systems Biology and Applications*, *10*(1), 18. https://doi.org/10.1038/s41540-024-00340-w

Filtz, T. M., Vogel, W. K., & Leid, M. (2014). Regulation of transcription factor activity by interconnected post-translational modifications. *Trends in Pharmacological Sciences*, *35*(2), 76–85. https://doi.org/10.1016/j.tips.2013.11.005

Franz, M., Lopes, C. T., Huck, G., Dong, Y., Sumer, O., & Bader, G. D. (2016). Cytoscape.js: A graph theory library for visualisation and analysis. *Bioinformatics (Oxford, England)*, *32*(2), 309–311.

Ge, W., Wang, Y., Quan, M., Mao, T., Bischof, E. Y., Xu, H., Zhang, X., Li, S., Yue, M., Ma, J., Yang, H., Wang, L., Yu, Z., Wang, L., & Cui, J. (2024). Activation of the PI3K/AKT signaling pathway by ARNTL2 enhances cellular glycolysis and sensitizes pancreatic adenocarcinoma to erlotinib. *Molecular Cancer*, *23*(1), 48. https://doi.org/10.1186/s12943-024-01965-5

Goldman, M. J., Craft, B., Hastie, M., Repečka, K., McDade, F., Kamath, A., Banerjee, A., Luo, Y., Rogers, D., Brooks, A. N., Zhu, J., & Haussler, D. (2020). Visualizing and interpreting cancer genomics data via the Xena platform. *Nature Biotechnology*, *38*(6), 675–678. https://doi.org/10.1038/s41587-020-0546-8

GTEx Consortium. (2013). The genotype-tissue expression (GTEx) project. *Nature Genetics*, *45*(6), 580–585. https://doi.org/10.1038/ng.2653

Hanahan, D. (2022). Hallmarks of cancer: New dimensions. *Cancer Discovery*, *12*(1), 31–46. https://doi.org/10.1158/2159-8290.CD-21-1059

Hanahan, D., & Weinberg, R. A. (2011). Hallmarks of cancer: The next generation. *Cell*, *144*(5), 646–674. https://doi.org/10.1016/j.cell.2011.02.013

Hartung, M., Anastasi, E., Mamdouh, Z. M., Nogales, C., Schmidt, H. H. H. W., Baumbach, J., Zolotareva, O., & List, M. (2022). Cancer driver drug interaction explorer. *Nucleic Acids Research*, *50*(W1), W138–W144. https://doi.org/10.1093/nar/gkac384

Huang, Y., Chang, X., Zhang, Y., Chen, L., & Liu, X. (2021). Disease characterization using a partial correlation-based sample-specific network. *Briefings in Bioinformatics*, *22*(3), bbaa062. https://doi.org/10.1093/bib/bbaa062

Huynh-Thu, V. A., Irrthum, A., Wehenkel, L., & Geurts, P. (2010). Inferring regulatory networks from expression data using tree-based methods. *PLoS ONE*, *5*(9), e12776. https://doi.org/10.1371/journal.pone.0012776

Inukai, S., Kock, K. H., & Bulyk, M. L. (2017). Transcription factor-DNA binding: Beyond binding site motifs. *Current Opinion in Genetics & Development*, *43*, 110–119. https://doi.org/10.1016/j.gde.2017.02.007

Jensen, L. J., Kuhn, M., Stark, M., Chaffron, S., Creevey, C., Muller, J., Doerks, T., Julien, P., Roth, A., Simonovic, M., Bork, P., & von Mering, C. (2009). STRING 8--a global view on proteins and their functional interactions in 630 organisms. *Nucleic Acids Research*, *37*(Database issue), D412–D416. https://doi.org/10.1093/nar/gkn760

Katsila, T., Spyroulias, G. A., Patrinos, G. P., & Matsoukas, M.-T. (2016). Computational approaches in target identification and drug discovery. *Computational and Structural Biotechnology Journal*, *14*, 177–184. https://doi.org/10.1016/j.csbj.2016.04.004

Keshamouni, V. G. (2018). Excavation of FOSL1 in the ruins of KRAS-driven lung cancer [review of *excavation of FOSL1 in the ruins of KRAS-driven lung cancer*]. *American Journal of Respiratory Cell and Molecular Biology*, *58*(5), 551–552.

Ketteler, A., & Blumenthal, D. B. (2023). Demographic confounders distort inference of gene regulatory and gene co-expression networks in cancer. *Briefings in Bioinformatics*, *24*(6), bbad413. https://doi.org/10.1093/bib/bbad413

Kim, H.-I., Lim, H., & Moon, A. (2018). Sex differences in cancer: Epidemiology, genetics and therapy. *Biomolecules & Therapeutics*, *26*(4), 335–342. https://doi.org/10.4062/biomolther.2018.103

Kim-Hellmuth, S., Aguet, F., Oliva, M., Muñoz-Aguirre, M., Kasela, S., Wucher, V., Castel, S. E., Hamel, A. R., Viñuela, A., Roberts, A. L., Mangul, S., Wen, X., Wang, G., Barbeira, A. N., Garrido-Martín, D., Nadel, B. B., Zou, Y., Bonazzola, R., Quan, J., … Lappalainen, T. (2020). Cell type-specific genetic regulation of gene expression across human tissues. *Science*, *369*(6509), eaaz8528. https://doi.org/10.1126/science.aaz8528

Kremer, L. S., Bader, D. M., Mertes, C., Kopajtich, R., Pichler, G., Iuso, A., Haack, T. B., Graf, E., Schwarzmayr, T., Terrile, C., Koňaříková, E., Repp, B., Kastenmüller, G., Adamski, J., Lichtner, P., Leonhardt, C., Funalot, B., Donati, A., Tiranti, V., … Prokisch, H. (2017). Genetic diagnosis of Mendelian disorders via RNA sequencing. *Nature Communications*, *8*(1), 15824. https://doi.org/10.1038/ncomms15824

Kuhn, H. W. (1955). The Hungarian method for the assignment problem. *Naval Research Logistics Quarterly*, *2*(1–2), 83–97. https://doi.org/10.1002/nav.3800020109

Kuijjer, M. L., Tung, M. G., Yuan, G., Quackenbush, J., & Glass, K. (2019). Estimating sample-specific regulatory networks. *IScience*, *14*, 226–240. https://doi.org/10.1016/j.isci.2019.03.021

Laconi, E., Marongiu, F., & DeGregori, J. (2020). Cancer as a disease of old age: Changing mutational and microenvironmental landscapes. *British Journal of Cancer*, *122*(7), 943–952. https://doi.org/10.1038/s41416-019-0721-1

Lambert, S. A., Jolma, A., Campitelli, L. F., Das, P. K., Yin, Y., Albu, M., Chen, X., Taipale, J., Hughes, T. R., & Weirauch, M. T. (2018). The human transcription factors. *Cell*, *172*(4), 650–665. https://doi.org/10.1016/j.cell.2018.01.029

Lee, H.-Y., Kim, H.-K., Hoang, T.-H., Yang, S., Kim, H.-R., & Chae, H.-J. (2020). The correlation of IRE1α oxidation with Nox4 activation in aging-associated vascular dysfunction. *Redox Biology*, *37*, 101727. https://doi.org/10.1016/j.redox.2020.101727

Lee, W., Huang, D.-S., & Han, K. (2020). Constructing cancer patient-specific and group-specific gene networks with multi-omics data. *BMC Medical Genomics*, *13*(Suppl 6), 81. https://doi.org/10.1186/s12920-020-00736-7

Link, J. C., Wiese, C. B., Chen, X., Avetisyan, R., Ronquillo, E., Ma, F., Guo, X., Yao, J., Allison, M., Chen, Y.-D. I., Rotter, J. I., El-Sayed Moustafa, J. S., Small, K. S., Iwase, S., Pellegrini, M., Vergnes, L., Arnold, A. P., & Reue, K. (2020). X chromosome dosage of histone demethylase KDM5C determines sex differences in adiposity. *The Journal of Clinical Investigation*, *130*(11), 5688–5702. https://doi.org/10.1172/JCI140223

Liu, C., Liu, L., Yang, M., Li, B., Yi, J., Ai, X., Zhang, Y., Huang, B., Li, C., Feng, C., & Zhou, Y. (2020). A positive feedback loop between EZH2 and NOX4 regulates nucleus pulposus cell senescence in age-related intervertebral disc degeneration. *Cell Division*, *15*, 2. https://doi.org/10.1186/s13008-020-0060-x

Liu, X., Wang, Y., Ji, H., Aihara, K., & Chen, L. (2016). Personalized characterization of diseases using sample-specific networks. *Nucleic Acids Research*, *44*(22), e164. https://doi.org/10.1093/nar/gkw772

Louadi, Z., Yuan, K., Gress, A., Tsoy, O., Kalinina, O. V., Baumbach, J., Kacprowski, T., & List, M. (2021). DIGGER: Exploring the functional role of alternative splicing in protein interactions. *Nucleic Acids Research*, *49*(D1), D309–D318. https://doi.org/10.1093/nar/gkaa768

Maier, A., Hartung, M., Abovsky, M., Adamowicz, K., Bader, G. D., Baier, S., Blumenthal, D. B., Chen, J., Elkjaer, M. L., Garcia-Hernandez, C., Helmy, M., Hoffmann, M., Jurisica, I., Kotlyar, M., Lazareva, O., Levi, H., List, M., Lobentanzer, S., Loscalzo, J., … Baumbach, J. (2024). Drugst. One—A plug-and-play solution for online systems medicine and network-based drug repurposing. *Nucleic Acids Research*, *52*, W481–W488. https://doi.org/10.1093/nar/gkae388

Margolin, A. A., Nemenman, I., Basso, K., Wiggins, C., Stolovitzky, G., Dalla Favera, R., & Califano, A. (2006). ARACNE: An algorithm for the reconstruction of gene regulatory networks in a mammalian cellular context. *BMC Bioinformatics*, *7*(S1), S7. https://doi.org/10.1186/1471-2105-7-S1-S7

Maron, B. A., Wang, R.-S., Shevtsov, S., Drakos, S. G., Arons, E., Wever-Pinzon, O., Huggins, G. S., Samokhin, A. O., Oldham, W. M., Aguib, Y., Yacoub, M. H., Rowin, E. J., Maron, B. J., Maron, M. S., & Loscalzo, J. (2021). Individualized interactomes for network-based precision medicine in hypertrophic cardiomyopathy with implications for other clinical pathophenotypes. *Nature Communications*, *12*(1), 873. https://doi.org/10.1038/s41467-021-21146-y

Mazzoccoli, G., Pazienza, V., Panza, A., Valvano, M. R., Benegiamo, G., Vinciguerra, M., Andriulli, A., & Piepoli, A. (2012). ARNTL2 and SERPINE1: Potential biomarkers for tumor aggressiveness in colorectal cancer. *Journal of Cancer Research and Clinical Oncology*, *138*(3), 501–511. https://doi.org/10.1007/s00432-011-1126-6

Nakazawa, M. A., Tamada, Y., Tanaka, Y., Ikeguchi, M., Higashihara, K., & Okuno, Y. (2021). Novel cancer subtyping method based on patient-specific gene regulatory network. *Scientific Reports*, *11*(1), 23653. https://doi.org/10.1038/s41598-021-02394-w

Nogales, C., Mamdouh, Z. M., List, M., Kiel, C., Casas, A. I., & Schmidt, H. H. H. W. (2022). Network pharmacology: Curing causal mechanisms instead of treating symptoms. *Trends in Pharmacological Sciences*, *43*(2), 136–150. https://doi.org/10.1016/j.tips.2021.11.004

Özdemir, B. C., & Dotto, G.-P. (2017). Racial differences in cancer susceptibility and survival: More than the color of the skin? *Trends in Cancer*, *3*(3), 181–197. https://doi.org/10.1016/j.trecan.2017.02.002

Park, B., Lee, W., Park, I., & Han, K. (2019). Finding prognostic gene pairs for cancer from patient-specific gene networks. *BMC Medical Genomics*, *12*(Suppl 8), 179. https://doi.org/10.1186/s12920-019-0634-0

Pearson, E. S. (1973). Tests for departure from normality. Empirical results for the distributions of b2 and √b1. *Biometrika*, *60*(3), 613–622.

Pedregosa, F., Varoquaux, G., Gramfort, A., Michel, V., Thirion, B., Grisel, O., Blondel, M., Louppe, G., Prettenhofer, P., Weiss, R., Weiss, R. J., Vanderplas, J., Passos, A., Cournapeau, D., Brucher, M., Perrot, M., & Duchesnay, E. (2011). Scikit-learn: Machine learning in Python. *Journal of Machine Learning Research: JMLR*, *12*(85), 2825–2830.

Phillips, T. (2008). The role of methylation in gene expression. *Nature Education*, *1*(1), 116.

Sadegh, S., Matschinske, J., Blumenthal, D. B., Galindez, G., Kacprowski, T., List, M., Nasirigerdeh, R., Oubounyt, M., Pichlmair, A., Rose, T. D., Salgado-Albarrán, M., Späth, J., Stukalov, A., Wenke, N. K., Yuan, K., Pauling, J. K., & Baumbach, J. (2020). Exploring the SARS-CoV-2 virus-host-drug interactome for drug repurposing. *Nature Communications*, *11*(1), 3518. https://doi.org/10.1038/s41467-020-17189-2

Sadegh, S., Skelton, J., Anastasi, E., Bernett, J., Blumenthal, D. B., Galindez, G., Salgado-Albarrán, M., Lazareva, O., Flanagan, K., Cockell, S., Nogales, C., Casas, A. I., Schmidt, H. H. H. W., Baumbach, J., Wipat, A., & Kacprowski, T. (2021). Network medicine for disease module identification and drug repurposing with the

NeDRex platform. *Nature Communications*, *12*(1), 6848. https://doi.org/10.1038/s41467-021-27138-2

Samanta, M. K., Gayen, S., Harris, C., Maclary, E., Murata-Nakamura, Y., Malcore, R. M., Porter, R. S., Garay, P. M., Vallianatos, C. N., Samollow, P. B., Iwase, S., & Kalantry, S. (2022). Activation of Xist by an evolutionarily conserved function of KDM5C demethylase. *Nature Communications*, *13*(1), 2602. https://doi.org/10.1038/s41467-022-30352-1

Sun, X., Frierson, H. F., Chen, C., Li, C., Ran, Q., Otto, K. B., Cantarel, B. L., Vessella, R. L., Gao, A. C., Petros, J., Miura, Y., Simons, J. W., & Dong, J.-T. (2005). Frequent somatic mutations of the transcription factor ATBF1 in human prostate cancer. *Nature Genetics*, *37*(4), 407–412. https://doi.org/10.1038/ng1528

Takaku, M., Grimm, S. A., De Kumar, B., Bennett, B. D., & Wade, P. A. (2020). Cancer-specific mutation of GATA3 disrupts the transcriptional regulatory network governed by estrogen receptor alpha, FOXA1 and GATA3. *Nucleic Acids Research*, *48*(9), 4756–4768. https://doi.org/10.1093/nar/gkaa179

Wang, Z., Liu, T., Xue, W., Fang, Y., Chen, X., Xu, L., Zhang, L., Guan, K., Pan, J., Zheng, L., Qin, G., & Wang, T. (2020). ARNTL2 promotes pancreatic ductal adenocarcinoma progression through TGF/BETA pathway and is regulated by miR-26a-5p. *Cell Death & Disease*, *11*(8), 692. https://doi.org/10.1038/s41419-020-02839-6

SUPPORTING INFORMATION

Additional supporting information can be found online in the Supporting Information section at the end of this article.

How to cite this article: Kersting, J., Lazareva, O., Louadi, Z., Baumbach, J., Blumenthal, D. B., & List, M. (2024). DysRegNet: Patient-specific and confounder-aware dysregulated network inference towards precision therapeutics. *British Journal of Pharmacology*, 1–16. https://doi.org/10.1111/bph.17395